Predicting mining collapse: Superjerks and the appearance of record-breaking events in coal as collapse precursors

Xiang Jiang,[1,2,3] Hanlong Liu,[1] Ian G. Main,[4] and Ekhard K. H. Salje[2,*]

[1]*School of Civil Engineering, Chongqing University, 400044 Chongqing, People's Republic of China*

[2]*Department of Earth Sciences, University of Cambridge, Downing Street, Cambridge CB2 3EQ, United Kingdom*

[3]*State Key Laboratory of Coal Mine Disaster Dynamics and Control, Chongqing University, 400044 Chongqing, People's Republic of China*

[4]*School of Geosciences, University of Edinburgh, Edinburgh EH9 3FE, United Kingdom*

(Received 23 February 2017; revised manuscript received 21 May 2017; published 9 August 2017)

The quest for predictive indicators for the collapse of coal mines has led to a robust criterion from scale-model tests in the laboratory. Mechanical collapse under uniaxial stress forms avalanches with a power-law probability distribution function of radiated energy $P \sim E^{-\varepsilon}$, with exponent $\varepsilon = 1.5$. Impending major collapse is preceded by a reduction of the energy exponent to the mean-field value $\varepsilon = 1.32$. Concurrently, the crackling noise increases in intensity and the waiting time between avalanches is reduced when the major collapse is approaching. These latter criteria were so-far deemed too unreliable for safety assessments in coal mines. We report a reassessment of previously collected extensive collapse data sets using "record-breaking analysis," based on the statistical appearance of "superjerks" within a smaller spectrum of collapse events. Superjerks are defined as avalanche signals with energies that surpass those of all previous events. The final major collapse is one such superjerk but other "near collapse" events equally qualify. In this way a very large data set of events is reduced to a sparse sequence of superjerks (21 in our coal sample). The main collapse can be anticipated from the sequence of energies and waiting times of superjerks, ignoring all weaker events. Superjerks are excellent indicators for the temporal evolution, and reveal clear nonstationarity of the crackling noise at constant loading rate, as well as self-similarity in the energy distribution of superjerks as a function of the number of events so far in the sequence $E_{sj} \sim n^{\delta}$ with $\delta = 1.79$. They are less robust in identifying the precise time of the final collapse, however, than the shift of the energy exponents in the whole data set which occurs only over a short time interval just before the major event. Nevertheless, they provide additional diagnostics that may increase the reliability of such forecasts.

DOI: 10.1103/PhysRevE.96.023004

I. INTRODUCTION

Jiang *et al.* [1] showed that the imminent collapse of coal mines is predictable by careful analysis of the acoustic emissions (AEs) of crackling noise during compression. This result was obtained by extensive laboratory experiments on samples obtained from anthracite coal seams. The criterion for imminent system-sized collapse was the reduction of the power-law exponents of the avalanche energy $P(E) \sim E^{-\varepsilon}$ from $\varepsilon = 1.5$ to $\varepsilon = 1.32$ (see [2,3] for nomenclature). A concurrent increase of the acoustic emission activity was equally observed when approaching the final failure event, which could also act as a "warning signal" for the impending major collapse. This increase relates to an increase of the emitted AE energy and the reduction of waiting times between subsequent signals. None of these effects were previously analyzed quantitatively. Note that we measure avalanche *energies* in our AE experiments, while some model calculations [4] use the more easily obtainable avalanche *amplitude*; for the close relation between these quantities see [2]. Strain intermittency due to avalanches in ferroelastic and porous materials has been studied for slowly increasing compressive uniaxial stress [5] for a large set of compounds. It was shown that some materials, such as charcoal, shale, and calcareous schist, also possess ε values bigger than the mean-field exponent $\varepsilon \cong 1.3$ [2].

Pál *et al.* [4] proposed to analyze the amplitude and waiting time of the AE signals and published the results of computer simulations of the collapse of porous materials. In their analysis they reduced the AE spectrum from the totality of all avalanche signals to a subset of "superjerks." A superjerk is defined as an avalanche signal with energy greater than any previous event of the series. Recently, such statistics of superjerks (also called "record-breaking" events) has attracted great attention due to its relevance for climate and earthquake research [6–9]. Related analytic results have been obtained for the statistics of the sequences of independent identically distributed (IID) random variables for a randomly sampled stationary process [9–11]. The statistics of "records" has previously been applied to understand correlated processes emerging in various types of random walks [12–14], superconductors [15], domain wall dynamics in spin glasses [16], and in chaotic processes [17]. The record statistics of the bursting activity has also been studied in models exhibiting self-organized criticality (SOC) [11] and in a mean-field model of fracture [18]. Record statistics were applied to reveal spatiotemporal clustering of seismicity either by focusing on the interevent times [9] or using both the spatial and temporal distance of events [7,8] during earthquakes. The experimental data of avalanche sequences in collapsing porous pillars of coal [1] show a similar increase of the AE energies as in simulations [4] so that it was tempting to reanalyze these data in terms of superjerks and record statistics. This analysis is important for other materials where the collapse under uniaxial stress equally showed the shift of the energy exponent and systematic

*Corresponding author: ekhard@esc.cam.ac.uk

changes of the AE activity and, sometimes, waiting times. These materials are shale [19], SiO_2 based minerals [3,20], berlinite [21], alumina [22], and goethite [23]. In no case was a quantitative analysis of superjerks undertaken.

We argue in this paper that the collapse of coal seams relates to two mechanisms, namely, the collapse around spatially isolated avalanches and, when the final collapse is imminent, the clustering of such avalanche localities along major fault lines. The two mechanisms are consistent with the existence of two separate populations of avalanches with distinct fixed-point exponents ε. We will discuss additional parameters of the superjerk analysis, which can be used as additional criteria for imminent collapse.

The analysis of shifting exponents appears different from traditional approaches where continuous evolutions are advocated [4]. The difference with [1] and the data given in this paper is likely due to the different selection criteria for sampling populations: The gradual changes of exponents reported in the literature may result from mixing of the fixed points allied to small sampling windows, both on a laboratory scale (as investigated here) and on a field scale (as demonstrated by Roberts *et al.* [24]) and are hence artifacts. Our much larger data set allows a full analysis of the collapse mechanism and a clear "early warning scenario" using the change of the energy exponent as indicator. It is also the purpose of this paper to describe the difference between continuous and abrupt changes of the energy of superjerks and the waiting time between subsequent superjerks and their assessment as additional indicators for imminent collapse.

II. ANALYSIS OF RECORD-BREAKING EVENTS: THE SUPERJERKS

Figure 1 shows the previously published AE events in coal samples undergoing deformation [uniaxial compression under constant stress rate, $d\sigma/dt = 8.5\,\mathrm{kPa/s}$ (1 kN/min)] in the laboratory. The coal samples' shapes were cylindrical with 50 mm diameter and 100 mm length. AE signals were measured during compression by two or more piezoelectric sensors fixed on the sample's round surface by rubber bands. The acoustic signal was preamplified (40 dB) and transferred to the AE analysis system. The threshold for detection was chosen as the threshold of an empty experiment (45 dB). More details are given in [1]. A total of 18 968 events were recorded. Statistical analysis showed that the data are power-law distributed $P(E) \sim E^{-\varepsilon}$ with energy exponents $\varepsilon = 1.5$ (early stage) and $\varepsilon = 1.32$ (late stage) [1]. As in most porous materials, we find that increasing strain loading triggers larger events so that the average burst size increases towards failure. We identify 21 superjerks in Fig. 1 as bursts with energies greater than any previous event. They are numbered by their "rank" $k = 1,2,\ldots,21$, namely, as the kth superjerk event of the complete time series, N_n is the number of superjerks in a given interval, and n counts the nth jerk in the full data set. Table I lists the detail data for superjerks in Fig. 1. Every superjerk has a rank k and is also the nth jerk. For example, the 12th superjerk ($k = 12$) is also the 681th jerk at a time $t_{12} = 18.123$ s with an energy 1 564 000 aJ (1 aJ $= 10^{-18}$ joules). Figure 1 illustrates that superjerks form a monotonically increasing subsequence of all jerks and divide

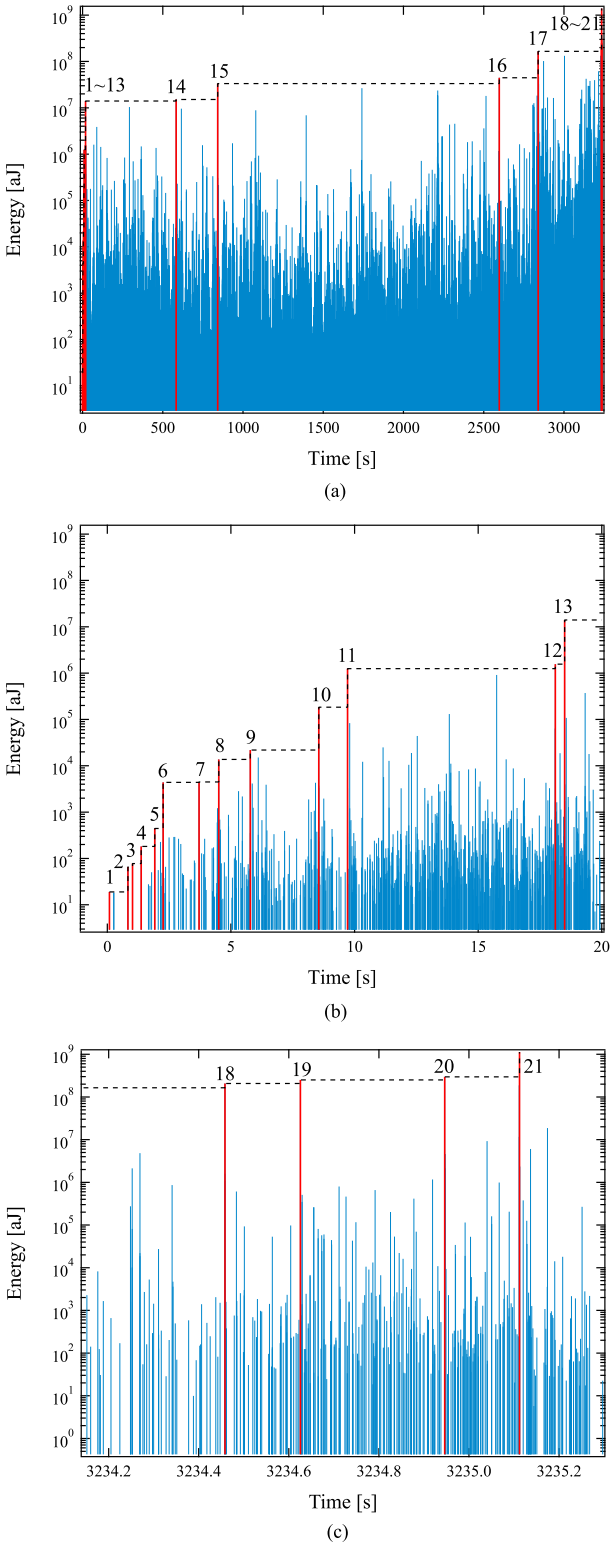

FIG. 1. Time sequence of jerk events in coal under uniaxial stress. The spectrum contains 18 968 jerks (blue) and 21superjerks as record-breaking events. Superjerks are more energetic than any of the previous jerks. (a) shows the full data set; (b), (c) are enlarged images for initial and last stages.

the time series into segments of varying number of smaller-size events. Table I also shows that the number of jerks between two subsequent superjerks is small until $k = 13$. For several

TABLE I. List of superjerks, their rank k, their equivalent jerk number n, their occurrence time t_k, and their energy E^k.

k	n	t_k (s)	E^k (aJ)
1	1	0.086888	18.96
2	5	0.8342943	65.80
3	6	1.0185958	77.48
4	7	1.3714062	182.14
5	11	1.9169895	445.36
6	17	2.2591618	4389.00
7	35	3.7108055	4484.00
8	50	4.5064265	13699.00
9	86	5.7838585	21850.00
10	169	8.552759	184309.00
11	200	9.715405	1254000.00
12	681	18.1231702	1564000.00
13	715	18.498928	14021000.00
14	3135	583.1427885	15059000.00
15	3827	842.1353625	33438000.00
16	8904	2596.877502	44600000.00
17	10578	2839.405836	165027000.00
18	18608	3234.458162	206865000.00
19	18656	3234.625663	251367000.00
20	18783	3234.94593	296159000.00
21	18858	3235.111935	1386000000.00

statistical analyses in the rest of the paper we focus on data with $k > 13$ because the statistical relevance of the data at $k < 13$ is too weak.

We observe, in accordance with Pál *et al.* [4], that the moving average of the event energy tends to increase near some superjerks (e.g., $k = 8$, 10, 11, 17 in Fig. 1), with a precursory increase in the average burst size, followed by a decrease after the superjerk has happened. To characterize how superjerks evolve during the loading process, we consider the energy increments δE^k and the waiting times m_k between consecutive superjerks defined as

$$\delta E^k = E^{k+1} - E^k, \tag{1}$$

$$m_k = t_{k+1} - t_k, \tag{2}$$

where E^k (t_k) is the energy (occurrence time) of the kth superjerk.

We now analyze the internal statistics of superjerks and compare them with the overall jerk statistics. The increasing average event energy and decreasing waiting time between consecutive events in Fig. 1 shows that the jerk series during collapse is highly nonstationary. The difference between stationary and nonstationary event series stems from the lack of correlations in stationary sequences and spatial and temporal correlations in nonstationary sequences [25–29]. It has been shown for sequences of independent identically distributed random variables that the statistics of record breakings has universal features [10]. The average number of superjerks $\langle N_n \rangle$ is calculated as follows: We identify all subsets of data with n events and find all superjerks in each of these subsets. For each value of n we identify the number of superjerks and average this number over all subsets. The average number of superjerks

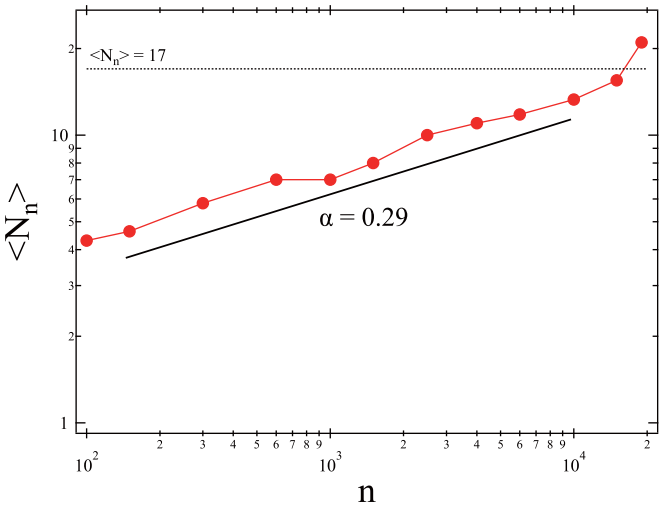

FIG. 2. Average number of superjerks $\langle N_n \rangle$ that occur before the nth jerk as a function of n (as double logarithmic plot). The line represents a power law with an exponent $\alpha = 0.29$. The relative increase of $\langle N_n \rangle$ at the highest value of n may be correlated with the occurrence of the superjerk with $k = 17$ which is indicated by the broken line.

grows in stationary series logarithmically with n:

$$\langle N_n \rangle \sim \kappa + \ln(n) + O\left(\frac{1}{n}\right) \quad \text{for} \quad n \to +\infty, \quad \kappa \approx 0.58. \tag{3}$$

This distribution is independent of the specific form of the probability density of the random variables [10]. In contrast, correlations between the nonstationary superjerks lead to power-law jerk statistics, with

$$\langle N_n \rangle \sim n^{\alpha}. \tag{4}$$

To identify the distribution $\langle N_n \rangle$ that applies for the collapse of coal samples, we plot the number of all superjerks with rank $\leqslant 21$. The sequences are not unique as it depends on the energy of the initial starting jerk. Starting from a jerk with a higher energy leads to a smaller number of superjerks. Only the largest series (starting at the first observable jerk of the 18 968 observed jerks) produces 21 superjerks; for all other series we used fixed windows for the intervals in n of 100, 150, 300, 600, 1000, 1500, 2500, 4000, 6000, 10 000, and 15 000 jerks.

The distribution is shown in Fig. 2 and shows a clear power law according to Eq. (4) with an exponent $\alpha = 0.29$. This value is in close agreement with the simulated value [4] of $\alpha = 0.33 \pm 0.03$ and shows that the collapse events in coals are indeed nonstationary, and do not occur in a random sequence as in Eq. (3), even in the early stages. A similar analysis in [4] showed deviations from the power law in the close vicinity of the final collapse. A weak increase of $\langle N_n \rangle$ (near 7 in [4]) also occurs in our data near $k = 17$ in Fig. 2.

The energy of superjerks E_{sj} equally depends on the number of jerks n that occur before the superjerk is triggered. Figure 3 shows that this distribution of energy is again a power law over eight decades in n. The power law is well described by

$$E_{sj} \sim n^{\delta} \quad \text{with} \quad \delta = 1.79.$$

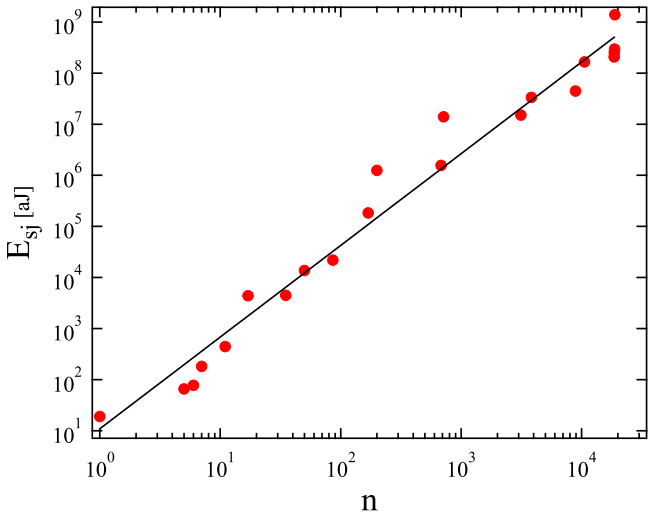

FIG. 3. Energy of superjerks E_{sj} after the nth jerk as a function of n on a double logarithmic scale. A power law $E_{sj} \sim n^{\delta}$ with $\delta = 1.79$ is found over a large energy scale of eight decades.

The energy distribution of superjerks is hence self-similar. In particular, changing the size of the system does not change the functional dependence on the total number of previously elapsed jerks before a superjerk is observed. The energy of superjerks for each rank k and the energy increment between two subsequent superjerks of rank k and $k-1$ (δE^k) are shown in Fig. 4. While this functional form is similar to that simulated in [4], the energy scale is much larger and spans seven decades. In this graph one can identify two regimes; namely, data at the early stages show a simple exponential increase of the energy of superjerks with increasing rank while those at the late stages saturate the energy. The crossover between the two regimes is also near $k = 17$ in Fig. 4. The big increment for the δE is caused by the final collapse containing a very large energy.

The systematic increase of the number of superjerks with the increasing number of jerks in Fig. 2 and the exponential

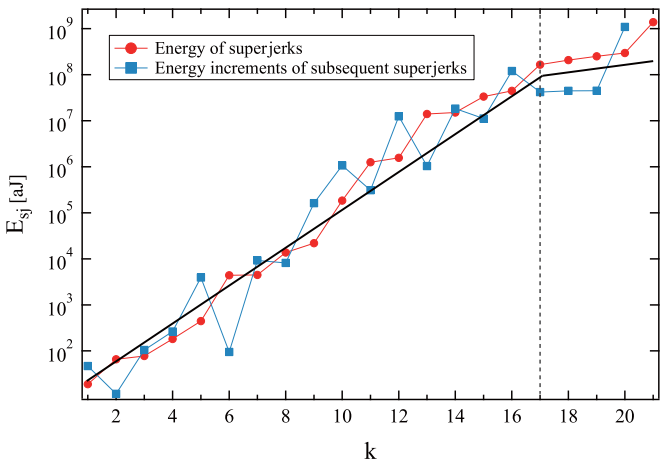

FIG. 4. Average value of the energy and the energy increment δE^k [see Eq. (1)] of superjerks as a function of the rank k. A weak break of slope occurs near $k = 17$.

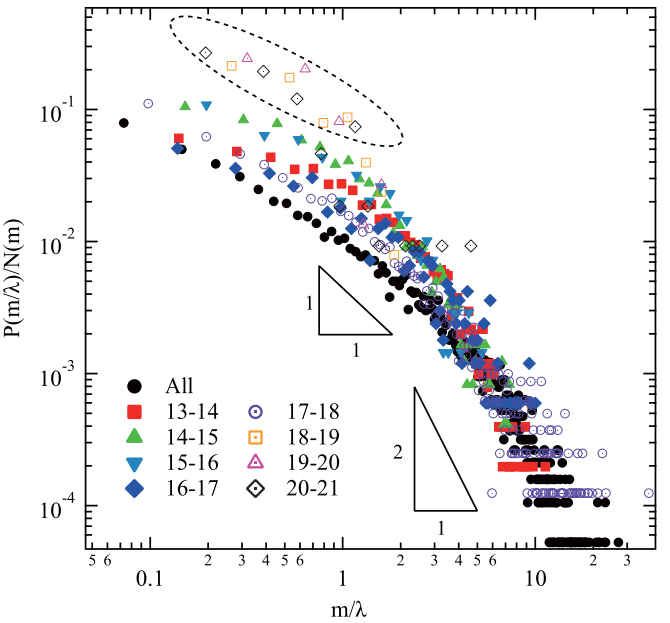

FIG. 5. Waiting time distribution functions for all events (black circles) and for jerks between superjerks. The data have been collapsed for large waiting times by a scaling factor λ. The probability distribution has been normalized by the total number of waiting times $N(m)$ which has been measured in each interval [bin size for each data set is twice the interquartile range divided by $N(m)^{1/3}$]. The (negative) exponents are near 2 for large waiting times and 1 for short waiting times, as indicated by the slopes of the triangles. Data for late events (18–21) in the dotted area show higher relative probabilities for short waiting times than all other curves.

increase of the energy of superjerks with increasing rank k in Fig. 4 precede the final collapse event. Simultaneously, the waiting times between jerks decreases with the approach to the final failure, indicating that avalanches do not only become more energetic but also succeed each other more rapidly when the structure approaches its final collapse. Similar behaviors have been reported for shale [19], granite [30], and gypsum [31] under uniaxial loading. The probability distribution function for the waiting time, $P(m) \sim m^{-(1-\nu)}$ for short waiting times and $P(m) \sim m^{-(2+\xi)}$ for long waiting times, was determined in [1] for the totality of all jerks. The exponents were $1-\nu \cong 1$ and $2+\xi \cong 2$ in agreement with previous observations [3,32]. We now analyze the same waiting time distributions for intervals between superjerks. We find that the maximum waiting times vary according to the time evolution of the interval between superjerks. Furthermore, the probability of a waiting time to occur is proportional to the number of data points in that interval. It is useful, therefore, to rescale the waiting time distributions by appropriate scaling factors. The results in Fig. 5 are hence collapsed first by a scaling factor λ that ensures that all curves coincide for long waiting times. The probability function $P(m/\lambda)$ is then normalized with respect to the total number of waiting times measured in each interval, $N(m)$. The collapse is excellent for long waiting times which demonstrates that the functional form of the rescales waiting time distribution is identical for all intervals between superjerks. The scaling

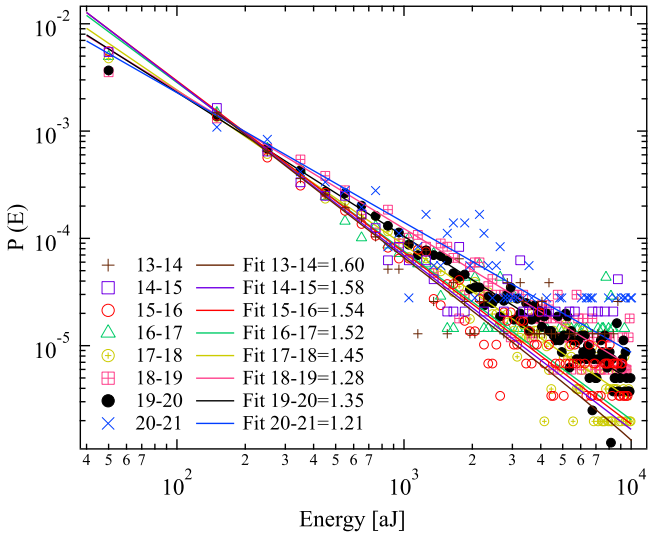

FIG. 6. Probability distribution functions $P(E)$ of AE energies for sequences of events between consecutive superjerks. Curves were fitted with simple power laws. The slopes of the curves correspond to the energy exponents. The number of bins is 100 with bin width 100 aJ for each subset.

factor λ then measures the time evolution of the waiting times over long time scales.

The collapse is indeed excellent for large waiting times but less good for short waiting times where jerks below the threshold may be missed in the analysis. Nevertheless, the higher value for the normalized probability function for the waiting times near the final collapse, 18–19, 19–20, 20–21, is obvious and shows that in this regime the jerks follow each other much more rapidly than for any interval with smaller rank k.

III. DISCUSSION

The main difference between our experimentally observed avalanche distributions and those of the simulations in [4] concerns the evolution of the energy or size exponent during the course of the experiment. While the experimentally observed changes of the energy exponent are relatively modest (1.5–1.32), simulations showed huge variations of the size exponent τ between 3.2 and 1, where "size" in [4] is defined by the number of broken bonds, as a proxy for source rupture area. The energy exponent is usually smaller than the size exponent (the conversion in mean-field theory is $(\tau - 1) = (\varepsilon - 1)(2 - \sigma \upsilon z)$ with $\sigma \upsilon z$ between 0 and 0.5) [2]), so we may estimate that the equivalent variation in the energy exponent is between 2.1–2.5 and 1. This is an unusually large range. To analyze this further we examine the PDFs of jerks in different time periods between the superjerks with ranks 13–14, 14–15, 15–16, 16–17, 17–18, 18–19, 19–20, and 20–21 (Fig. 6). In these intervals we have two or more orders of magnitude bandwidth of energy, and can hence have more confidence in an underlying power law. We determine the energy exponents for each power-law distribution and find a decrease with increasing rank from 1.6 to 1.21, which spans the values seen for coarser subsets [1], namely, from 1.5 to 1.32. In a like-for-like comparison with [4] for equivalent ranks, the equivalent range for τ is 2.0–1.0, and for ε is 1.67–1.0, closer to the results presented here. This highlights the importance of sampling over a wide bandwidth in determining power-law behavior, but leaves an outstanding question of the discrepancy at low implied values for ε in the model of [4].

All of the curves in Fig. 6 intersect near the energy 200 aJ. This makes all superpositions and mixing of power-law distributions effectively also power law with intermediate values of the energy exponent (Fig. 6). A linear behavior was observed over four decades of probability and two in energy, so the distribution of energies follows a power law in a good approximation:

$$P(E)dE \sim \frac{E^{-\varepsilon}}{E_{\min}^{1-\varepsilon}} dE \; E > E_{\min}, \tag{5}$$

where $E_{\min}$ is a lower cutoff needed for normalization (and experimentally unavoidable). In order to examine the distribution in more detail we apply the method presented in [33]. For discrete systems, we use the equation for the energy

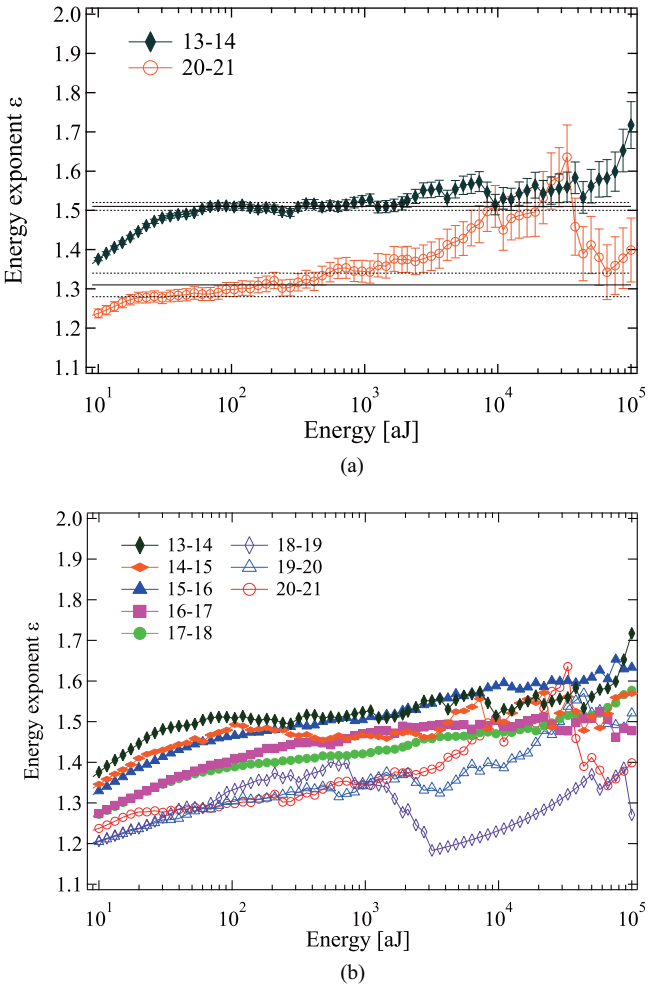

FIG. 7. Energy exponent as a function of the lower energy cutoff recorded determined by ML. (a) Energy exponents determined by the ML method for k intervals 13–14 and 20–21 with error bars and estimate values; (b) energy exponents for all intervals between $k = 13$ and $k = 21$. Sparse data sets lead to less well defined plateaus. We used data near 10^3 aJ to determine the energy exponents.

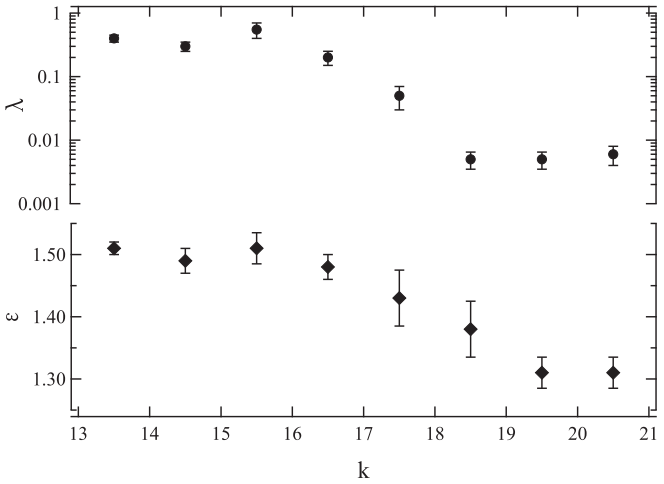

FIG. 8. Evolution of the waiting time renormalization factor λ and the energy exponent ε with increasing rank k of superjerks. Two plateaus can be distinguished for large and small λ and exponents near $\varepsilon = 1.5$ and $\varepsilon = 1.32$.

exponent,

$$\varepsilon(x_{\min}) = 1 + n\left[\sum_{i=1}^{n} \ln \frac{x_i}{x_{\min}}\right]^{-1}, \tag{6}$$

where x_i, $i = 1, \ldots, n$ are the observed values of x such that $x_i \geqslant x_{\min}$ a standard error

$$\sigma = \frac{\varepsilon(x_{\min}) - 1}{\sqrt{n}} + O\left(\frac{1}{n}\right). \tag{7}$$

The technique consists of studying the behavior of the power-law exponent ε determined using the maximum likelihood (ML) method, as a function of a varying lower cutoff $E_{\min}$. As shown in [1] this analysis leads to the two exponents $\varepsilon = 1.5$ and $\varepsilon = 1.32$. We analyze the data for intervals between superjerks (Fig. 7) and obtain power-law exponents as values of the onsets of the plateaus. These values vary between 1.5 and 1.32 in agreement with the previous assessment [1]. The evolution of the energy exponent with increasing rank k is shown in Fig. 8. These data are based on the height of the first plateau in the ML curves in Fig. 7. Higher values of the onset lead to the usual large fluctuations due to experimental noise [4].

Figure 8 shows that the largest energy exponents ε occur at the early stages and the smallest values near the final collapse. The crossover is found near the rank $k = 17$ where the jerk events are very sparse and the experimental uncertainties are particularly large [1]. The crossover behavior does not necessarily mean that no intermediate values of ε exist. Instead, a simple superposition of avalanche signals from the two regimes would mimic exactly such intermediate values of the energy exponent, even though the probability distribution function is not strictly a power law. It is easy to verify that such superpositions of two power laws with similar exponents yield functions that deviate from the power law by less than the experimental resolution. The results in Fig. 8 fully agree with the conclusions in [1]. Moreover, the scaling factor of the waiting time λ shows a similar behavior as ε, which can also be used to forecast the final collapse.

We now return to the assessment of the usefulness of a statistical analysis of superjerks for the prediction of major collapse events in coal mines and in laboratory experiments. The possible indicators are the appearance of superjerks and the reduction of waiting times near the major collapse event. We do indeed observe both phenomena. Their predictive power appears to be different, however. The appearance of superjerks shows a nonstationary evolution towards catastrophe. This criterion is insufficient for an early-warning signal, because the increase of the energy of superjerks is continuous and does not constitute a "critical" interval just before the major collapse.

Superjerks are useful, however, in order to break the evolution into smaller segments. Intervals between superjerks contain sufficient information to identify the approaching final collapse. The first weak effect is the change of slope in Fig. 4, which may identify an interval of criticality after the 17th superjerk. A second, much stronger warning is the reduction of the waiting times in the same interval in Fig. 8. It is correct, therefore, to identify the impending disaster by the sudden decrease of waiting times between jerks and a weak increase of the jerk energies. The most robust criterion is, nevertheless, the reduction of the energy exponent as argued in [1]. However, the criteria identified here from analyses of record-breaking events may provide additional diagnostics that may increase the reliability of such forecasts.

ACKNOWLEDGMENTS

X.J. acknowledges financial support from National Science and Technology Major Projects (Grant No. 2016ZX05045001-005); X.J. and H.L. acknowledge financial support from the National Natural Science Foundation of China (Grant No. 51678094). E.K.H.S. is grateful to EPSRC (Grants No. EP/K009702/1 and No. EP/P024904/1) for support. X.J. was supported by a scholarship from the China Scholarship Council to visit the University of Cambridge.

[1] X. Jiang, D. Jiang, J. Chen, and E. K. H. Salje, Am. Mineral. **101**, 2751 (2016).
[2] E. K. H. Salje and K. A. Dahmen, Annu. Rev. Condens. Matter Phys. **5**, 233 (2014).
[3] G. F. Nataf, P. O. Castillo-Villa, J. Baró, X. Illa, E. Vives, A. Planes, and E. K. H. Salje, Phys. Rev. E **90**, 022405 (2014).
[4] G. Pál, F. Raischel, S. Lennartz-Sassinek, F. Kun, and I. G. Main, Phys. Rev. E **93**, 033006 (2016).
[5] V. Soprunyuk, S. Puchberger, A. Tröster, E. Vives, E. K. H. Salje, and W. Schranz, J. Phys.: Condens. Matter **29**, 224002 (2017).
[6] G. Wergen and J. Krug, Europhys. Lett. **92**, 30008 (2010).

[7] J. Davidsen, P. Grassberger, and M. Paczuski, Geophys. Res. Lett. **33**, l11304 (2006).
[8] J. Davidsen, P. Grassberger, and M. Paczuski, Phys. Rev. E **77**, 066104 (2008).
[9] M. R. Yoder, D. L. Turcotte, and J. B. Rundle, Nonlin. Proc. Geophys. **17**, 169 (2010).
[10] G. Wergen, J. Phys. A: Math. Theor. **46**, 223001 (2013).
[11] R. Shcherbakov, J. Davidsen, and K. F. Tiampo, Phys. Rev. E **87**, 052811 (2013).
[12] S. N. Majumdar and R. M. Ziff, Phys. Rev. Lett. **101**, 050601 (2008).
[13] S. N. Majumdar, G. Schehr, and G. Wergen, J. Phys. A: Math. Theor. **45**, 355002 (2012).
[14] C. Godreche, S. N. Majumdar, and G. Schehr, J. Phys. A: Math. Theor. **47**, 255001 (2014).
[15] L. P. Oliveira, H. J. Jensen, M. Nicodemi, and P. Sibani, Phys. Rev. B **71**, 104526 (2005).
[16] H. J. Jensen, Adv. Solid State Phys. **45**, 95 (2006).
[17] S. C. L. Srivastavaa and A. Lakshminarayan, Chaos, Solitons Fractals **74**, 67 (2015).
[18] Z. Danku and F. Kun, Sci. Rep. **3**, 2688 (2013).
[19] J. Baró, A. Planes, E. K. H. Salje, and E. Vives, Philos. Mag. **96**, 3686 (2016).
[20] E. K. H. Salje, D. E. Soto-Parra, A. Planes, E. Vives, M. Reinecker, and W. Schranz, Philos. Mag. **91**, 554 (2011).
[21] G. F. Nataf, P. O. Castillo-Villa, P. Sellappan, W. M. Kriven, E. Vives, A. Planes, and E. K. H. Salje, J. Phys.: Condens. Matter **26**, 275401 (2014).
[22] P. O. Castillo-Villa, J. Baró, A. Planes, E. K. H. Salje, P. Sellappan, W. M. Kriven, and E. Vives, J. Phys.: Condens. Matter **25**, 292202 (2013).
[23] E. K. H. Salje, G. I. Lampronti, D. E. Soto-Parra, J. Baró, A. Planes, and E. Vives, Am. Mineral. **98**, 609 (2013).
[24] N. S. Roberts, A. F. Bell, and I. G. Main, Geophys. Res. Lett. **43**, 2011 (2016).
[25] T. P. Peixoto, K. Doblhoff-Dier, and J. Davidsen, J. Geophys. Res. **115**, B10309 (2010).
[26] J. B. Rundle, D. L. Turcotte, R. Shcherbakov, W. Klein, and C. Sammis, Rev. Geophys. **41**, 5 (2003).
[27] R. Albert and A. L. Barabasi, Rev. Mod. Phys. **74**, 47 (2002).
[28] F. Kun, I. Varga, S. Lennartz-Sassinek, and I. G. Main, Phys. Rev. Lett. **112**, 065501 (2014).
[29] K. Mair, I. Main, and S. Elphick, J. Struct. Geol. **22**, 25 (2000).
[30] V.Rudajeva, J.Vilhelma, and T. Lokajíăek, Int. J. Rock Mech. Min. **37**, 699 (2000).
[31] D. Chen, E. Wang, and N. Li, J. Geophys. Eng. **14**, 780 (2017).
[32] J. Baró, Á. Corral, X. Illa, A. Planes, E. K. H. Salje, W. Schranz, D. E. Soto-Parra, and E. Vives, Phys. Rev. Lett. **110**, 088702 (2013).
[33] A. Clauset, C. Shalizi, and M. Newman, SIAM Rev. **51**, 661 (2009).